ELSEVIER

Physica B 205 (1995) 183–192

PHYSICA B

Effect of phonon scattering on free-carrier absorption in n-type indium antimonide films

Chhi-Chong Wu[a,*], Chau-Jy Lin[b]

[a]*Institute of Electronics, National Chiao Tung University, Hsinchu, Taiwan*
[b]*Department of Applied Mathematics, National Chiao Tung University, Hsinchu, Taiwan*

Received 15 March 1994; revised 27 July 1994

Abstract

The free-carrier absorption in n-type InSb films has been investigated for carriers confined in quasi-two-dimensional (2D) semiconductors with the nonparabolic energy band of electrons. We discuss the effect of phonon scattering on the free-carrier absorption coefficient (α) for both deformation-potential coupling and piezoelectric coupling. α is found to depend on the photon polarization relative to the direction normal to the quasi-2D structure, the photon frequency, the film thickness, and the temperature. α could be complex due to the interaction between photons, phonons, and electrons. (i) When the acoustic phonon scattering is dominant, α increases with decreasing the film thickness for phonons polarized parallel or perpendicular to the layer plane. It is also shown that α increases with decreasing photon frequency and increasing temperature for photons polarized parallel to the layer plane, while for photons polarized perpendicular to the layer plane the α temperature-dependence is more complicated. (ii) If the piezoelectric scattering is dominant, α is also decreasing with increasing the film thickness for photons polarized parallel or perpendicular to the layer plane. But α decreases with increasing temperature for photons polarized perpendicular to the layer plane. Moreover, numerical results for the parallel polarization are much smaller than those for the perpendicular polarization.

1. Introduction

There has been a growing interest in the electronic and optical properties of semiconducting layered heterojunctions [1–6], thin films [7, 8], and inversion layers [9–11]. Due to the confinement of carriers in these quasi-two-dimensional structures, size quantization begins to play an important role in determining their electronic and optical properties. The optical absorption can take place via direct interband transitions, and intersubband transitions, and indirect intraband transitions in which the carriers absorb or emit a photon while simultaneously scattering off phonons or other imperfections. Such free-carrier absorption accounts for absorption of photons with frequency Ω lower than the band gap E_g of semiconductors, i.e., $\hbar\Omega < E_g$. In a magnetic field, where the carrier motion is confined to a plane perpendicular to the magnetic field, the free-carrier absorption coefficient (α) depends upon the photon polarization relative to the magnetic field [12]. For carriers confined in a quasi-2D structure, it was found that α depends upon the photon polarization relative to

* Corresponding author.

0921-4526/95/$09.50 © 1995 Elsevier Science B.V. All rights reserved
SSDI 0921-4526(94)00618-0

the direction normal to the quasi-2D structure [13]. In III–V semiconductors, the acoustic-phonon–carrier interaction is dominated by the deformation-potential and piezoelectric couplings [14].

In this paper, we investigate the quantum theory of the free-carrier absorption in III–V semiconductors with the nonparabolic energy band of electrons with a quasi-2D structure. It has been shown that the nonparabolicity of the energy band in semiconductors can be used to explain the longitudinal magnetoacoustic phenomenon [15] and the acoustic-surface-wave amplification [14]. In this calculation, we consider a nondegenerate electron gas with a Maxwell–Boltzmann distribution for nondegenerate semiconductors. Thus, we make following assumptions:

(1) For a nondegenerate semiconductor, the distribution function of electrons can be represented by the Maxwell–Boltzmann distribution. The effect of Fermi energy can be neglected for the nondegenerate electron gas in a nondegenerate semiconductor [13].

(2) The interaction between electrons and acoustic phonons originates from the deformation-potential and piezoelectric couplings in III–V semiconductors.

(3) The energy band of electrons in semiconductors is assumed to be of nonparabolicity.

In Section 2, we recall the electronic states of a quasi-2D structure for the nonparabolic band structure. In Section 3, we present the quantum theory of the free-carrier absorption with confined carriers in nondegenerate semiconductors for the deformation-potential and piezoelectric couplings. We discuss two special cases: the photon is polarized parallelly or perpendicularly to the layer plane. In Section 4, some numerical results of the free-carrier absorption coefficient are presented for n-type InSb. Finally, a brief discussion about our numerical analysis is given.

2. Electronic states in a thin semiconductor layer

The motion of conduction electrons parallel to the thin films may be described by plane waves, and those perpendicular to the surface will be described by the type of standing waves depending on the structure of potential. For a square well potential along the z axis with infinitely high barriers at $z = 0$ and $z = d$, the electron field operator $\Psi^\dagger(\boldsymbol{r})$ is given [16] by

$$\Psi^\dagger(\boldsymbol{r}) = \left(\frac{2}{V}\right)^{1/2} \sum_{n=1}^{\infty} \sum_{\boldsymbol{k}} b^\dagger_{\boldsymbol{k}n} \exp(-\mathrm{i}\boldsymbol{k}\cdot\boldsymbol{x}) \sin\left(\frac{n\pi z}{d}\right), \tag{1}$$

where $\boldsymbol{r} = (\boldsymbol{x}, z) = (x, y, z)$, $V = dS$ is the film volume, S being the surface area, and d the film thickness, $\boldsymbol{k} = (k_x, k_y)$ is the electron wave vector in the x–y plane, and $b^\dagger_{\boldsymbol{k}n}$ is the electron creation operator. The electron energy $E_{\boldsymbol{k}n}$ is given [14, 17–19] by the relation

$$\varepsilon_{\boldsymbol{k}n} = E_{\boldsymbol{k}n}\left(1 + \frac{E_{\boldsymbol{k}n}}{E_g}\right) = \frac{\hbar^2 \boldsymbol{k}^2}{2m^*} + \frac{\pi^2\hbar^2 n^2}{2m^* d^2}, \quad n = 1, 2, 3, \ldots, \tag{2}$$

where m^* is the effective mass and $\varepsilon_{\boldsymbol{k}n}$ is the effective eigenvalue due to the effective Hamiltonian [19]. The electron energy for the nonparabolic band $E_{\boldsymbol{k}n}$ in Eq. (2) can be written as

$$E_{\boldsymbol{k}n} = -\tfrac{1}{2}E_g\left\{1 - \left[1 + \left(\frac{4}{E_g}\right)\left(\frac{\hbar^2\boldsymbol{k}^2}{2m^*} + \frac{\pi^2\hbar^2 n^2}{2m^* d^2}\right)\right]^{1/2}\right\} \quad n = 1, 2, 3, \ldots \tag{3}$$

Since $(\hbar^2 k^2_{\max})/2m^* + (\pi\hbar n)^2/2m^* d^2 \cong k_B T < E_g$ for $T \leqslant 300\,\mathrm{K}$, Eq. (3) can be expanded as

$$E_{\boldsymbol{k}n} \cong -\tfrac{1}{2}E_g + \tfrac{1}{2}E_g a_n + \hbar^2\boldsymbol{k}^2/2m^* a_n \tag{4}$$

$$\text{with} \quad a_n = [1 + (2\pi^2\hbar^2 n^2)/(m^* d^2 E_g)]^{1/2}. \tag{5}$$

In the case of low photon energies, the electron energies received from the photons are also small. Thus only low quantum numbers will contribute to the system. Thus we may expand a_n from Eq. (5) for the second term of Eq. (4) and obtain the expression

$$E_{\boldsymbol{k}n} \cong \frac{\pi^2\hbar^2 n^2}{2m^* d^2} + \frac{\hbar^2\boldsymbol{k}^2}{2m^*_n} \tag{6}$$

with $m^*_n = m^* a_n$. This expression for $E_{\boldsymbol{k}n}$ is almost the same type as shown in Ref. [19]. In our present work, we consider any values of photon energies, and the energy received by electrons is not so small. Hence we use the nonparabolic band of electrons as

shown in Eq. (4). It is seen that Eq. (6) can be reduced to the parabolic band of electrons in semiconductors as the parameter a_n is taken to a limit one. Since the quantum number n cannot be zero, thus the parabolic band of electrons is only a limit model of the nonparabolic band of electrons in III–V semiconductors.

3. Quantum theory of free-carrier absorption in quasi-2D nondegenerate semiconductors

The absorption coefficient α for the absorption of photons can be expressed [13] as

$$\alpha = \frac{\varepsilon^{1/2}}{n_0 c} \sum_i W_i f_i, \tag{7}$$

where ε is the dielectric constant of material, n_0 is the number of photons in the radiation field, f_i is the distribution function of carriers and W_i is the transition probability. It is given with the Born approximation

$$W_i = \frac{2\pi}{\hbar} \sum_f \left[|\langle f | M_+ | i \rangle|^2 \delta(E_f - E_i - \hbar\Omega - \hbar\omega_q) + |\langle f | M_- | i \rangle|^2 \delta(E_f - E_i - \hbar\Omega + \hbar\omega_q) \right], \tag{8}$$

where E_i and E_f are the initial and final electron energies, $\hbar\Omega$ is the photon energy, $\hbar\omega_q$ is the phonon energy. For interaction between electrons, photons, and phonons, the transition matrix elements $\langle f | M_\pm | i \rangle$ are given by

$$\langle f | M_\pm | i \rangle = \sum_j \left[\frac{\langle f | H_{\mathrm{rad}} | j \rangle \langle j | V_{\mathrm{s}} | i \rangle}{E_j - E_i \mp \hbar\omega_q} + \frac{\langle f | V_{\mathrm{s}} | j \rangle \langle j | H_{\mathrm{rad}} | i \rangle}{E_j - E_i - \hbar\Omega} \right], \tag{9}$$

where H_{rad} is the electron–photon interaction and V_{s} is the scattering potential due to the electron–phonon interaction.

The electron–photon interaction is given by

$$H_{\mathrm{rad}} = -\frac{e}{m^*} \left(\frac{2\pi\hbar n_0}{\varepsilon \Omega V} \right)^{1/2} \boldsymbol{\varepsilon} \cdot \boldsymbol{p}, \tag{10}$$

where $\boldsymbol{\varepsilon}$ is the photon polarization vector and $\boldsymbol{p}$ is the electron momentum. Its matrix elements for electrons in the same band are given as follows:

(i) When the photon is polarized parallelly to the layer plane,

$$\langle \boldsymbol{k}'n' | H_{\mathrm{rad}} | \boldsymbol{k}n \rangle = -\frac{e}{m^*} \left(\frac{2\pi\hbar n_0}{\varepsilon \Omega V} \right)^{1/2} \boldsymbol{\varepsilon} \cdot (\hbar \boldsymbol{k}) \delta_{n',n} \delta_{k_x', k_x} \delta_{k_y', k_y}. \tag{11}$$

(ii) When the photon is polarized perpendicularly to the layer plane,

$$\langle \boldsymbol{k}'n' | H_{\mathrm{rad}} | \boldsymbol{k}n \rangle = -\frac{ie\hbar}{m^*} \left(\frac{2\pi\hbar n_0}{\varepsilon \Omega V} \right)^{1/2} \left(\frac{n}{d} \right) \times \left\{ \frac{1 - \cos[\pi(n' + n)]}{n' + n} + \frac{1 - \cos[\pi(n' - n)]}{n' - n} \right\} \times \delta_{k_x', k_x} \delta_{k_y', k_y}. \tag{12}$$

The distribution function for a quasi-2D nondegenerate electron gas in nondegenerate semiconductors can be expressed as

$$f_{\boldsymbol{k}n} = \left(\frac{n_{\mathrm{e}} d \hbar^2}{2\pi^2 m^* k_{\mathrm{B}} T} \right)^{1/2} \left[\sum_{l=1}^{\infty} a_l \exp\left(-\frac{E_{\mathrm{g}} a_l}{2 k_{\mathrm{B}} T} \right) \right]^{-1} \times \exp\left[-\frac{E_{\mathrm{g}} a_n}{2 k_{\mathrm{B}} T} - \frac{\hbar^2 \boldsymbol{k}^2}{2 m^* k_{\mathrm{B}} T a_n} \right], \tag{13}$$

where n_{e} is the concentration of electrons.

For III–V semiconductors, there are two dominant electron–phonon scattering mechanisms:

3.1. *Deformation-potential coupling*

When the deformation-potential coupling is dominant, the electron–phonon potential [18, 20] reads

$$V_{\mathrm{s}} = \left(\frac{k_{\mathrm{B}} T}{2 \rho v_{\mathrm{s}}^2 V} \right)^{1/2} E_{\mathrm{d}} \exp(\mathrm{i} \boldsymbol{q} \cdot \boldsymbol{r}), \tag{14}$$

where ρ is the density of material, v_{s} is the sound velocity, $\boldsymbol{q}$ is the phonon wave vector, and E_{d} is the deformation potential. For wave functions given in

Eq. (1), one can have

$$\langle \boldsymbol{k}'n'|V_s|\boldsymbol{k}n\rangle = \frac{1}{2}\left(\frac{k_B T}{2\rho v_s^2 V}\right)^{1/2} E_d \delta_{k'_x, k_x+q_x}\delta_{k'_y, k_y+q_y} \times [\delta_{q_z, (\pi/d)(n'-n)} + \delta_{q_z, -(\pi/d)(n'-n)} - \delta_{q_z, (\pi/d)(n'+n)} - \delta_{q_z, -(\pi/d)(n'+n)}]. \quad (15)$$

From Eqs. (7)–(9), (11)–(13) and (15), the free-carrier absorption coefficient for a quasi-2D electron gas can be obtained as shown in Appendix. From Eqs. (A.1) and (A.7), it can be seen that the free-carrier absorption coefficient could be complex coming from the logarithmic functions due to the interaction between electrons, photons and phonons.

3.2. Piezoelectric coupling

When the piezoelectric coupling is dominant, the electron–phonon potential is given [18] by

$$V_s = \left(\frac{k_B T}{2\rho v_s^2 V}\right)^{1/2} \frac{|e|\beta_P}{\varepsilon q} \exp(i\boldsymbol{q}\cdot\boldsymbol{r}) \quad (16)$$

where β_P is the appropriate piezoelectric constant. For wave functions given in Eq. (1), one can have

$$\langle \boldsymbol{k}'n'|V_s|\boldsymbol{k}n\rangle = \frac{1}{2}\left(\frac{k_B T}{2\rho v_s^2 V}\right)^{1/2} \frac{|e|\beta_P}{\varepsilon q} \delta_{k'_x, k_x+q_x} \times \delta_{k'_y, k_y+q_y}[\delta_{q_z, (\pi/d)(n'-n)} + \delta_{q_z, -(\pi/d)(n'-n)} - \delta_{q_z, (\pi/d)(n'+n)} - \delta_{q_z, -(\pi/d)(n'+n)}]. \quad (17)$$

From Eqs. (7)–(9), (11)–(13) and (17), the free-carrier absorption coefficient for a quasi-2D electron gas can be obtained as in Appendix. From Eqs. (A.12) and (A.15), it can also be seen that the free-carrier absorption coefficient could be complex coming from the logarithmic functions in there due to the interaction between electrons, photons, and phonons.

4. Numerical analysis and discussion

In this section, a numerical example is developed for an n-type nondegenerate InSb thin film. The relevant values of physical parameters are taken to be [15, 21] $n_e = 1.75\times10^{14}\,\mathrm{cm}^{-3}$, $m^* = 0.013m_0$ (m_0 is the free electron mass), $\rho = 5.8\,\mathrm{gm/cm^3}$, $\varepsilon = 18$, $E_g = 0.2\,\mathrm{eV}$, $E_d = 4.5\,\mathrm{eV}$, $\beta_P = 1.8\times10^4$ $\mathrm{esu/cm^2}$ and $v_s = 4\times10^5\,\mathrm{cm/s}$.

4.1. Deformation-potential coupling

In Fig. 1(a), the free-carrier absorption coefficient in n-type InSb films is plotted as a function of the photon frequency with $d = 10\,\mu\mathrm{m}$ for photons polarized parallelly to the layer plane. Since the real and imaginary parts of α have the same order of numerical values, $|\alpha|$ appears monotonically decreasing with increasing the photon frequency [22]. It can also be seen that $|\alpha|$ increases with temperature. We plot the free-carrier absorption coefficient in n-type InSb films as a function of the photon frequency with $d = 10\,\mu\mathrm{m}$ for photons polarized perpendicularly to the layer plane as shown in Fig. 1(b). Since the imaginary part of α is quite small compared with the real part of α, hence $\alpha \cong |\alpha|$ for this case [22]. It can be seen that α decreases with increasing the photon frequency. However, the changing of α with temperature appears irregularly in lower frequencies with $\Omega < 25\,\mathrm{THz}$ at higher temperatures such as $T = 77$ and $300\,\mathrm{K}$. In Fig. 2(a), we plot the free-carrier absorption coefficient as a function of the film thickness with the photon frequency $\Omega = 28\,\mathrm{THz}$ (or $10.6\,\mu\mathrm{m}$ wavelength of CO_2 laser) for photons polarized parallelly to the layer plane. It is shown that $|\alpha|$ decreases with increasing the film thickness and increases with temperature. In Fig. 2(b), we plot the free-carrier absorption coefficient as a function of the film thickness with $\Omega = 28\,\mathrm{THz}$. Since the imaginary part of α appears some significant values only with $d < 0.4\,\mu\mathrm{m}$ except at $T = 4.2\,\mathrm{K}$ in which the imaginary part of α vanishes [22], thus it can also be approximated as $\alpha \cong |\alpha|$ except $T = 4.2\,\mathrm{K}$. It is shown that α decreases with increasing the film thickness. However, the changing of α with temperature does not appear in a regular trend. Some small oscillations of the free-carrier absorption coefficient with the changing of the film thickness demonstrate the confinement of electrons in these quasi-two-dimensional structures. This phenomenon is coming from the interaction between

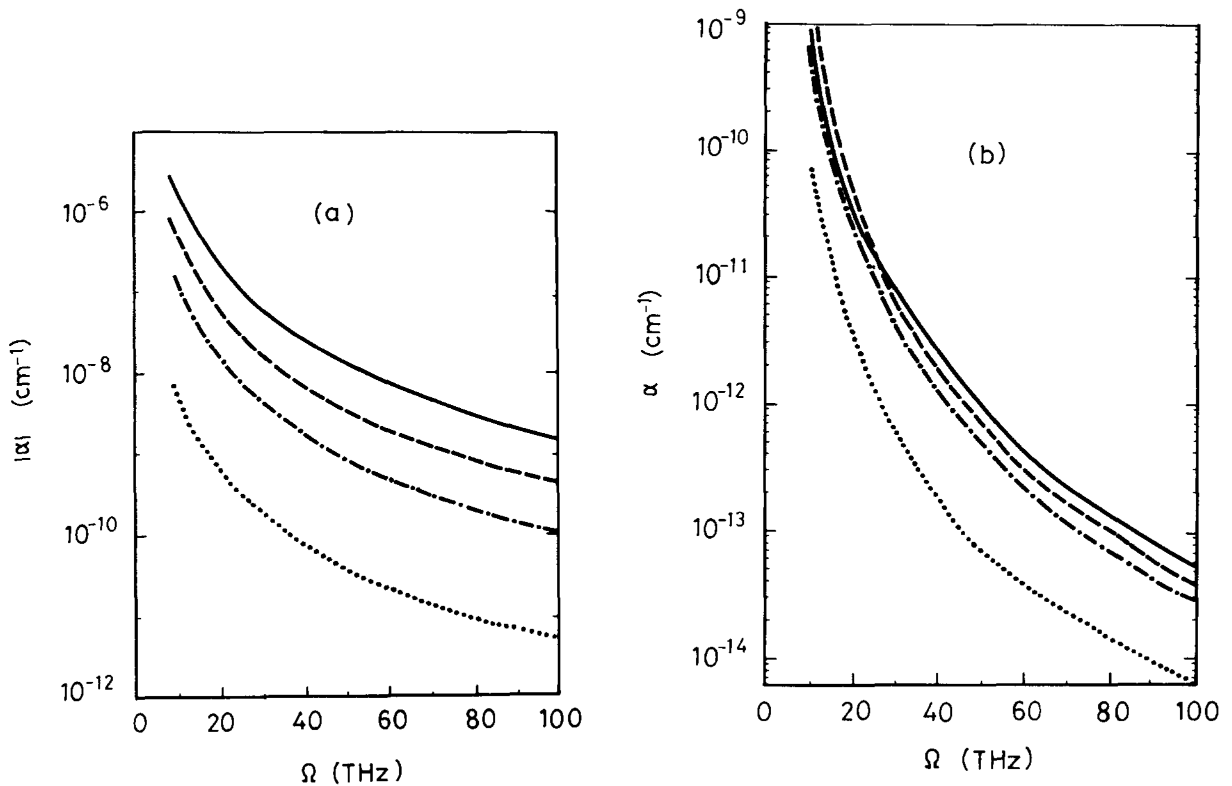

Fig. 1. Free-carrier absorption coefficient in n-InSb films due to acoustic phonon coupling as a function of photon frequency with $d = 10\,\mu m$ for photons polarized (a) parallel and (b) perpendicular to the layer plane for various temperatures: $T = 300\,K$ (——), $T = 77\,K$ (– – –), $T = 19.7\,K$ (–·–·–), and $T = 4.2\,K$ (······).

photons, phonons, and electrons in nondegenerate semiconductors.

4.2. Piezoelectric coupling

We plot the free-carrier absorption coefficient in n-type InSb films as a function of the photon frequency with $d = 10\,\mu m$ for photons polarized parallel to the layer plane as shown in Fig. 3(a). Since the values of the imaginary part of α are quite small compared to those of the real part of α [22], thus $\alpha \cong |\alpha|$. It can be seen that α decreases monotonically with increasing the photon frequency and increases with temperature. While for photons polarized perpendicularly to the layer plane as shown in Fig. 3(b), it is shown that α decreases monotonically with increasing the photon frequency, but α decreases with increasing temperature. This is different from that in Fig. 3(a) for photons polarized parallel to the layer plane. For this case, the imaginary part of α appears quite small compared with the real part of α in the order of 10^{-6} [22]. In Fig. 4(a), the free-carrier absorption coefficient is plotted as a function of the film thickness with $\Omega = 28\,THz$ (or $10.6\,\mu m$ wavelength of CO_2 laser) for photons polarized parallel to the layer plane. It can be seen that α decreases monotonically with increasing the film thickness and also increases with temperature. In Fig. 4(b), we plot the free-carrier absorption coefficient as a function of the film thickness for photons polarized perpendicularly to the layer plane with $\Omega = 28\,THz$ (or $10.6\,\mu m$ wavelength of CO_2 laser). It can be seen that in low temperatures α decreases monotonically with increasing the film thickness. But α decreases with increasing temperature after the film thickness

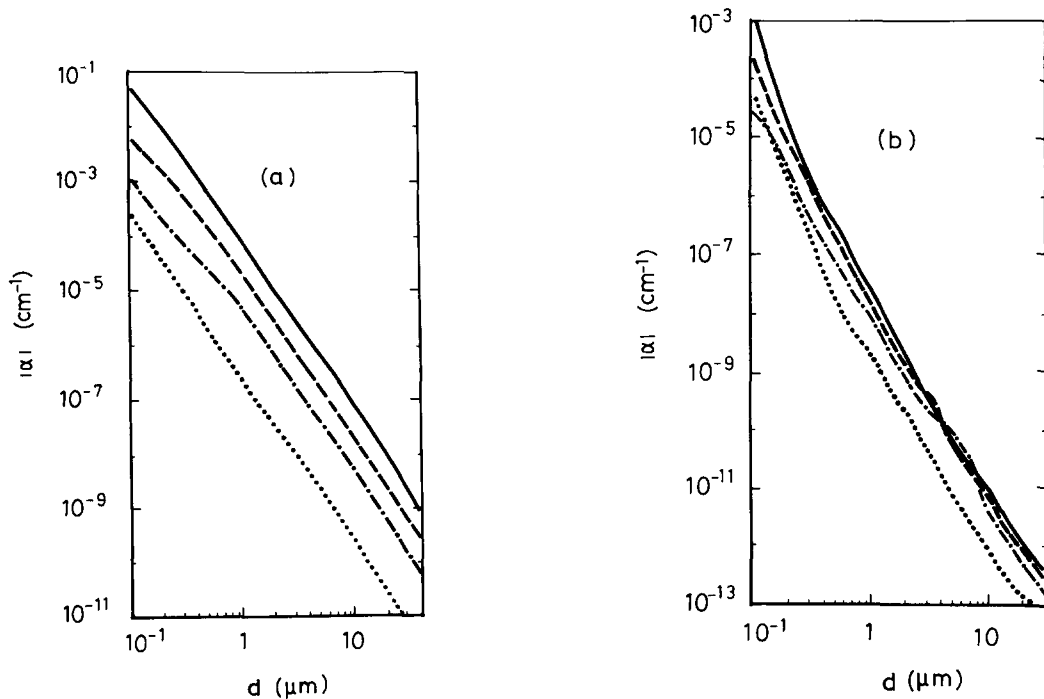

Fig. 2. Free-carrier absorption coefficient in n-InSb films due to acoustic phonon coupling as a function of the film thickness with $\Omega = 28$ THz for photons polarized (a) parallel and (b) perpendicular to the layer plane for various temperatures: $T = 300$ K (——), $T = 77$ K (– – –), $T = 19.7$ K (–·–·–·–), and $T = 4.2$ K (·······).

$d = 3 \times 10^{-1}$ μm. This is different from that Fig. 4(a). However, at higher temperatures such as $T = 77$ and 300 K, α oscillates with the film thickness in a region of small thickness of films, $d < 3 \times 10^{-1}$ μm, and then decreases monotonically with increasing the film thickness. This is coming from the fact that there exists a cusp minimum point in the real part of α and there are some oscillations in the imaginary part of α in the region $d < 3 \times 10^{-1}$ μm [22]. Moreover, the real and imaginary parts of α in this region appear the same order of numerical values. After passing this region, the imaginary part of α drops abruptly and discontinuously to a quite small value compared with the real part of α as $T = 77$ and 300 K for the effect of phonons becoming more considerably.

From our numerical results presented here, it is shown that the free-carrier absorption coefficient in n-type InSb films depends upon the photon polarization, the photon frequency, the film thickness, and the temperature. When the acoustic phonon scattering is dominant, the free-carrier absorption coefficient appears irregular dependence on temperature for photons polarized perpendicularly to the layer plane. However, when the piezoelectric scattering is dominant, the free-carrier absorption coefficient increases with decreasing temperature for photons polarized perpendicularly to the layer plane. Thus the dependence of temperature on the free-carrier absorption coefficient for the piezoelectric scattering is quite different from that for the deformation-potential scattering in this kind of polarization. We have also shown that the effect of the nonparabolicity of electrons in semiconductors will be relevant at high electron energy and thus a high photon energies. At low frequencies the parabolic band of electrons is a reasonable approximation. The deviation for the approximation at low frequencies will be from

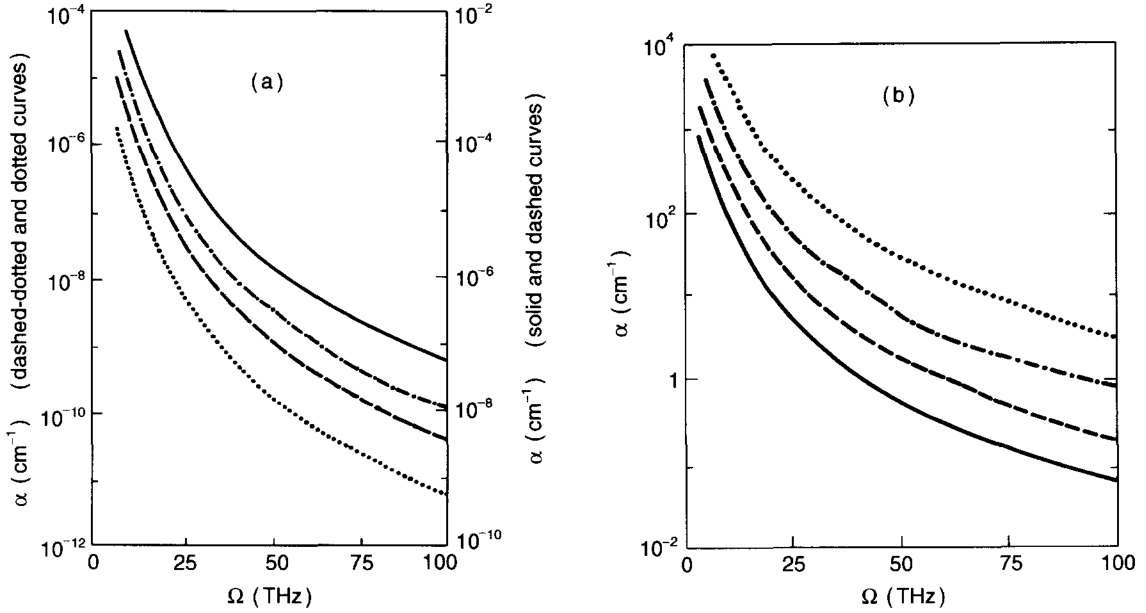

Fig. 3. Free-carrier absorption coefficient in n-InSb films due to piezoelectric coupling as a function of photon frequency with $d = 10\,\mu\text{m}$ for photons polarized (a) parallel and (b) perpendicular to the layer plane for various temperatures: $T = 300\,\text{K}$ (——), $T = 77\,\text{K}$ (– – –), $T = 19.7\,\text{K}$ (–·–·–·–), and $T = 4.2\,\text{K}$ (·······).

Eqs. (4)–(6) as

$$\Delta E_{kn} = \frac{\pi^2\hbar^4 k^2 n^2}{2m^{*2}d^2E_g}. \tag{18}$$

This is very small if we take a limit $n = 1$.

Acknowledgement

This study was supported by National Science Council, Republic of China, under contract number: NSC-81-0404-E009-539.

Appendix

Deformation-potential coupling

(i) When the photon is polarized parallel to the layer plane,

$$\alpha = \alpha_D\left[\sum_{l=1}^{\infty} a_l \exp\left(-\frac{a_l}{2\tau}\right)\right]^{-1}\sum_{n_i=1}^{\infty}\sum_{n_f}^{N_f} a_{n_i}\exp\left(-\frac{a_{n_i}}{2\tau}\right)$$
$$\times\left\{k_T^2 d^2 a_{n_i}\left[-\frac{1}{4}\ln\left(\frac{U_{if}^+}{U_{if}^-}\right)+\frac{1}{8}(U_{if}^-)^{-1}\right.\right.$$
$$\left.-\frac{1}{8}(U_{if}^+)^{-1}+4\gamma n_i n_f\right]+\pi^2\gamma^{-1}\left[\frac{3}{16}\ln\left(\frac{U_{if}^+}{U_{if}^-}\right)\right.$$
$$-\frac{1}{4}\gamma\sum_{\lambda=-1}^{+1}{}'\,\lambda(n_f+\lambda n_i)^2\ln\left(\frac{4}{3}U_{if}^{\lambda}\right)$$
$$\left.\left.+\frac{1}{32}\sum_{\lambda=-1}^{+1}{}'\,\lambda(U_{if}^{\lambda})^{-1}+\frac{1}{3}\gamma n_i n_f\right]\right\}, \tag{A.1}$$

where

$$\alpha_D = \frac{2\pi^4 e^2 n_e k_B T E_d^2}{\Omega^3\varepsilon^{1/2}\rho v_s^2 m^* c d^3\hbar^2}, \tag{A.2}$$

$$\gamma = \left(\frac{\pi v_s}{d\Omega}\right)^2, \tag{A.3}$$

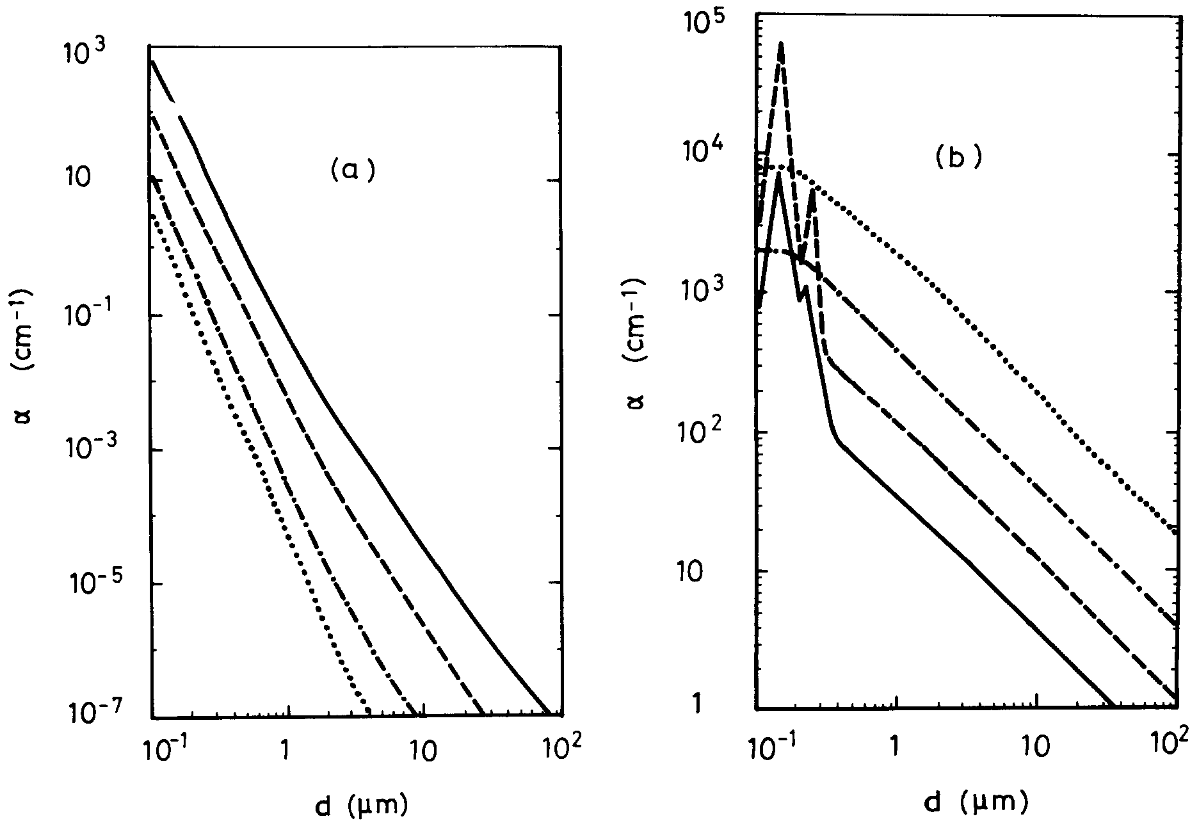

Fig. 4. Free-carrier absorption coefficient in n-InSb films due to piezoelectric coupling as a function of the film thickness with $\Omega = 28$ THz for photons polarized (a) parallel and (b) perpendicular to the layer plane for various temperatures: $T = 300$ K (——), $T = 77$ K (– – –), $T = 19.7$ K (–·–·–·–), and $T = 4.2$ K (·······).

$$k_B T = \tau E_g = \frac{\hbar^2 k_T^2}{2m^*}, \tag{A.4}$$

$$U_{if}^{\pm} = \gamma (n_f \pm n_i)^2 - \frac{1}{4} \tag{A.5}$$

and N_f can be determined from

$$n_i < N_f \leqslant n_i + d\Omega/\pi v_s. \tag{A.6}$$

(ii) When the photon is polarized perpendicularly to the layer plane,

$$\alpha = \alpha_D \left[\sum_{l=1}^{\infty} a_l \exp\left(-\frac{a_l}{2\tau} \right) \right]^{-1} \sum_{n_i=1}^{\infty} \sum_{n_f=1}^{N_f} \sum_{n'=1}^{N'} (n')^2 \times a_{n_i} \left[\frac{1 - \cos \pi (n_f + n')}{n_f + n'} + \frac{1 - \cos \pi (n_f - n')}{n_f - n'} \right]^2$$

$$\times \exp\left(-\frac{a_{n_i}}{2\tau} \right) \left\{ \sum_{\lambda=-1}^{+1}{}' \ln \left(\frac{V_{if}'^{+} + \lambda E_{if}'}{V_{if}'^{-} + \lambda E_{if}'} \right) + \sum_{\mu=-1}^{+1}{}' \sum_{\lambda=-1}^{+1}{}' [V_{if}'^{\mu} - \lambda] \exp[\lambda V_{if}'^{\mu} - E_{if}'] \times E_i[-\lambda V_{if}'^{\mu} + E_{if}'] \right\}, \tag{A.7}$$

where

$$V_{if}'^{\pm} = \left(\frac{\pi v_s \hbar}{d k_B T} \right) (n' \pm n_i)(a_{n_f} + a_{n'})(a_{n_f} - a_{n'}), \tag{A.8}$$

$$E_{if}' = \left(\frac{E_g}{2 k_B T} \right) \left(\frac{a_{n_i} a_{n'} + a_{n_f}^2 - a_{n'}^2 - a_{n_i} a_{n_f}}{a_{n_f} - a_{n'}} \right) - \frac{\hbar \Omega a_{n_f}}{k_B' T (a_{n_f} - a_{n'})} \tag{A.9}$$

and the exponential-integral function $E_i(x)$ is defined [23, 24] as

$$E_i(x) = -\int_x^{\infty} \frac{e^{-t}}{t}\,dt = \int_{-\infty}^{x} \frac{e^t}{t}\,dt. \tag{A.10}$$

N' and N_f are determined from

$$n_i < N' < N_f \leqslant n_i + d\Omega/\pi v_s. \tag{A.11}$$

Piezoelectric coupling

(i) When the photon is polarized parallel to the layer plane,

$$\begin{aligned}\alpha = {} & \alpha_P \left[\sum_{l=1}^{\infty} a_l \exp\left(-\frac{a_l}{2\tau}\right)\right]^{-1} \sum_{n_i=1}^{\infty} \sum_{n_f=1}^{N_f} a_{n_i} \\ & \times \exp\left(-\frac{a_{n_i}}{2\tau}\right)\left\{\frac{2m^* d^2 \gamma k_B T a_{n_i}}{\pi^2\hbar^2}\left[8\ln\left(\frac{n_f+n_i}{n_f-n_i}\right)\right.\right. \\ & \left. - 3\ln\left(\frac{U_{if}^+}{U_{if}^-}\right) - \sum_{\lambda=-1}^{+1}{}' \frac{\lambda}{2}(U_{if}^{\lambda})^{-1}\right] \\ & + 2\gamma n_i n_f \ln[16U_{if}^+U_{if}^-] - 8\gamma n_i n_f\left[\frac{1}{2}\ln(\gamma) + \frac{1}{3}\right] \\ & - 2\gamma \sum_{\lambda=-1}^{+1}{}' \lambda(n_f+\lambda n_i)^2 \ln(n_f+\lambda n_i) \\ & \left. - 4(\ln 3)\gamma n_i n_f + \frac{1}{4}[1 + 4\gamma(n_f^2+n_i^2)]\ln\left(\frac{U_{if}^+}{U_{if}^-}\right)\right\}\end{aligned} \tag{A.12}$$

where

$$\alpha_P = \frac{2\pi^6 e^4 n_e k_B T \beta_P^2}{\Omega^3 \varepsilon^{5/2} \rho v_s^2 m^* c d^3 \hbar^2} \tag{A.13}$$

and N_f can be determined from

$$n_i < N_f \leqslant n_i + d\Omega/\pi v_s. \tag{A.14}$$

(ii) When the photon is polarized perpendicularly to the layer plane,

$$\begin{aligned}\alpha = {} & \alpha_P\left(\frac{\gamma\hbar^2\Omega^2}{k_B T \pi^2}\right)\left[\sum_{l=1}^{\infty} a_l \exp\left(-\frac{a_l}{2\tau}\right)\right]^{-1} \\ & \times \sum_{n_i=1}^{\infty}\sum_{n_f=1}^{N_f}\sum_{n'=1}^{N'} \frac{(n')^2 a_{n_i} a_{n'}^2}{(a_{n_f}-a_{n'})^2}\left[\frac{1-\cos\pi(n_f+n')}{n_f+n'}\right. \\ & \left. + \frac{1-\cos\pi(n_f+n')}{n_f-n'}\right]^2 \exp\left(-\frac{a_{n_i}}{2\tau}\right) \\ & \times\left\{2\ln\left(\frac{n'+n_i}{n'-n_i}\right)\left[(k_B T)^{-1}\exp\left(\frac{K'_{if}}{k_B T}\right)E_i\left(-\frac{K'_{if}}{k_B T}\right)\right.\right. \\ & \left. - (K'_{if})^{-1} + \sum_{\lambda=-1}^{+1}{}' \sum_{\mu=-1}^{+1}{}' \lambda P[K'_{if}, \mu W_{if}'^{\lambda}]\right] \\ & \left. + (a_{n_f} - a_{n'})\sum_{\lambda=-1}^{+1}{}' \lambda Q[K'_{if}, W_{if}'^{\lambda}]\right\},\end{aligned} \tag{A.15}$$

where

$$K'_{if} = \hbar\Omega a_{n_f}(a_{n_f}-a_{n'})^{-1} - \tfrac{1}{2}E_g(a_{n_i}a_{n'} + a_{n_f}^2 - a_{n'}^2 - a_{n_i}a_{n_f})(a_{n_f}-a_{n'})^{-1}, \tag{A.16}$$

$$W_{if}'^{\pm} = (\pi\hbar v_s/d)(n' \pm n_i)(a_{n_f}+a_{n'})(a_{n_f}-a_{n'})^{-1}, \tag{A.17}$$

$$\begin{aligned}P(K,V) = {} & -k_B T\left\{\left[5 - 2\ln\left(\frac{2m^* a_{n_i} d^2 V}{\pi^2\hbar^2}\right)\right]K^{-1}\right. \\ & \times(K+V)^{-1} + \left[2 - 2\ln\left(\frac{4m^{*2}a_{n_i}^2 d^4 KV}{\pi^2\hbar^4}\right)\right. \\ & \left. + \ln\left(\frac{2m^* a_{n_i} d^2 K}{\pi^2\hbar^2}\right)\ln\left(\frac{2m^* a_{n_i} d^2 V}{\pi^2\hbar^2}\right)\right](K+V)^{-2} \\ & + \left[\ln\left(\frac{2m^* a_{n_i} d^2 V}{\pi^2\hbar^2}\right) - 1\right] \\ & \left. \times\ln\left[\frac{2m^* a_{n_i} d^2 (K+V)}{\pi^2\hbar^2}\right]K^{-2}\right\} \\ & + \left[1 - \ln\left(\frac{4m^{*2}a_{n_i}^2 d^2 KV}{\pi^4\hbar^4}\right)\right](K+V)^{-1} \\ & - (2k_B T K^{-2} - K^{-1})\exp\left(\frac{V}{k_B T}\right)E_i\left(-\frac{V}{k_B T}\right) \\ & + V^{-1}\exp\left(\frac{K}{k_B T}\right)E_i\left(-\frac{K}{k_B T}\right) \\ & + (k_B T)^{-1}\exp\left(\frac{K+V}{k_B T}\right)E_i\left(-\frac{V}{k_B T}\right) \\ & - \left\{3K^{-1} + V^{-1} - (k_B T)^{-1}\ln\left(\frac{4m^{*2}a_{n_i}^2 d^4 KV}{\pi^4\hbar^4}\right)\right.\end{aligned}$$

$$- 2k_BTK^{-2}\Big\}\exp\left(\frac{K+V}{k_BT}\right)E_i\left(-\frac{K+V}{k_BT}\right) \quad (A.18)$$

and

$$Q(K,V) = V^{-1}\left\{\exp\left(\frac{K+V}{k_BT}\right)E_i\left(-\frac{K+V}{k_BT}\right) - \exp\left(\frac{K-V}{k_BT}\right)E_i\left(-\frac{K-V}{k_BT}\right)\right\}, \quad (A.19)$$

N' and N_f can be determined from

$$n_i < N' < N_f \leqslant n_i + d\Omega/\pi v_s. \quad (A.20)$$

The sums over λ or μ with Σ' indicate $\lambda, \mu = -1$ to $+1$ without 0. For the notation for λ or μ, $+1$ means " + ", and -1 means " − ".

References

[1] L.L. Chang, L. Esaki and R. Tsu, Appl. Phys. Lett. 24 (1974) 593.
[2] R. Dingle, W. Wiegmann and C.H. Henry, Phys. Rev. Lett. 33 (1974) 827.
[3] L. Esaki and L.L. Chang, Phys. Rev. Lett. 33 (1974) 495.
[4] R. Dingle, A.C. Grossard and W. Wiegmann, Phys. Rev. Lett. 34 (1975) 1327.
[5] A.C. Seabaugh, W.R. Frensley, J.N. Randall, M.A. Reed, D.L. Farrington and R.J. Matyi, IEEE Trans. Electron Devices 36 (1989) 2328.
[6] S.M. Chudinov, V.A. Kul'bachinskii, G. Mancini, B.K. Medvedev and D.Yu. Rodichev, Fiz. Tekh. Poluprovodn. 24 (1990) 1905 [Sov. Phys.-Semicond. 24 (1990) 1185].
[7] D.C. Mattis and G. Beni, Phys. Rev. B 18 (1978) 3816.
[8] C.C. Wu and J. Tsai, Appl. Phys. Lett. 42 (1983) 535.
[9] G.D. Mahan and J.J. Hopfield, Phys. Rev. 135 (1965) A485.
[10] H. Esawa, Ann. Phys. NY 67 (1971) 438.
[11] S. Padmanabhan and A. Rothwarf, IEEE Trans. Electron Devices 36 (1989) 2557.
[12] T.M. Rynne and H.N. Spector, J. Appl. Phys. 52 (1981) 393.
[13] H.N. Spector, Phys. Rev. B 28 (1983) 971.
[14] C.C. Wu, Phys. Rev. B 28 (1983) 7094.
[15] C.C. Wu and H.N. Spector, Phys. Rev. B 3 (1971) 3979.
[16] S. Tamura and T. Sakuma, Phys. Rev. B 16 (1977) 3936.
[17] E.O. Kane, J. Phys. Chem. Solids 1 (1957) 249.
[18] B.R. Nag, Theory of Electrical Transport in Semiconductors (Pergamon Press, Oxford, 1972) p. 214.
[19] G. Bastard, J.A. Brum and R. Ferreira, Solid State Physics, Vol. 44 (Academic Press, New York, 1991) p. 229.
[20] J. Blatt, Physics of Electronic Conduction in Solids (McGraw-Hill, New York, 1968) p. 170.
[21] C.C. Wu and A. Chen, Phys. Rev. B 18 (1978) 1916.
[22] C.C. Wu, Report of National Science Council of China in Taiwan, 1993, unpublished.
[23] I.S. Gradshteyn and I.M. Ryzhik, Table of Integrals, Series, and Products (Academic Press, New York, 1965).
[24] M. Abramowitz and I.A. Stegun, Handbook of Mathematical Functions with Formulas, Graphs, and Mathematical Tables (National Bureaus of Standards, Washington, DC, 1968).